All-electron CI calculations of 3d transition-metal $L_{2,3}$ XANES using zeroth-order regular approximation for relativistic effects

2009 J. Phys.: Condens. Matter 21 104209

(http://iopscience.iop.org/0953-8984/21/10/104209)

J. Phys.: Condens. Matter **21** (2009) 104209 (5pp) doi:10.1088/0953-8984/21/10/104209

All-electron CI calculations of 3d transition-metal $L_{2,3}$ XANES using zeroth-order regular approximation for relativistic effects

Yu Kumagai[1], **Hidekazu Ikeno**[1] **and Isao Tanaka**[1,2]

[1] Department of Materials Science and Engineering, Kyoto University, Yoshida, Sakyo, Kyoto 606-8501, Japan
[2] Nanostructures Research Laboratory, Japan Fine Ceramics Centre, Atsuta, Nagoya 456-8587, Japan

E-mail: yuu@t01.mbox.media.kyoto-u.ac.jp

Received 31 October 2008, in final form 11 December 2008
Published 10 February 2009
Online at stacks.iop.org/JPhysCM/21/104209

Abstract

X-ray-absorption near-edge structures (XANES) at 3d transition-metal (TM) $L_{2,3}$ edges are computed using the all-electron configuration interaction (CI) method. Slater determinants for the CI calculations are composed of molecular orbitals obtained by density functional theory (DFT) calculations of model clusters. Relativistic effects are taken into account by the zeroth-order regular approximation (ZORA) using two-component wavefunctions. The theoretical spectra are found to be strongly dependent on the quality of the one-electron basis functions. On the other hand, a different choice of the exchange–correlation functionals for the DFT calculations does not exhibit visible changes in the spectral shape. Fine details of multiplet structures in the experimental TM $L_{2,3}$ XANES of MnO, FeO and CoO are well reproduced by the present calculations when the one-electron basis functions are properly selected. This is consistent with our previous report showing good agreement between theoretical and experimental TM $L_{2,3}$ XANES when four-component relativistic wavefunctions were used.

1. Introduction

3d transition-metal (TM) compounds play major roles in modern material science and engineering, such as diluted magnetic semiconductors and colossal magnetoresistive materials. X-ray-absorption near-edge structures (XANES) at TM $L_{2,3}$ edges, which mainly correspond to the electronic dipole transitions of $2p_{1/2}$ and $2p_{3/2}$ core electrons to unoccupied 3d orbitals, are quite useful to investigate the electronic and magnetic states of 3d electrons [1–12]. In order to interpret experimental spectra, theoretical spectra are often utilized as fingerprints. It is well known that the 3d TM $L_{2,3}$ XANES cannot be reproduced by a single-particle method such as band calculations based on density functional theory (DFT). Because of the strong inter-electron interactions among the core hole, excited electron and 3d electrons, the TM $L_{2,3}$ XANES is strongly modified from the empty 3d density of states. This is known as the multiplet effect. In order to treat the excitation from core orbitals, the relativistic effects should be considered. Recently the present authors' group has developed a first-principles many-electron method to calculate TM $L_{2,3}$ XANES using a fully relativistic configuration interaction method (CI) [7–12]. The CI calculations were made as a post-self-consistent field (SCF) process. We have demonstrated that it successfully reproduced the experimental spectra including fine structures. It has already been applied to some realistic problems, for example, to the study on the local structures of Mn impurities in GaN and Ga_2O_3 [13, 14] Charge states of Ni oxides were identified by a combination of Ni $L_{2,3}$ electron-energy-loss near-edge structures (ELNES) with such calculations. ELNES obtained by transmission electron microscopy reflects the same electronic transition as that of XANES [10].

In the present study, we examine the dependence of theoretical TM $L_{2,3}$ XANES on the quality of the basis sets and exchange–correlation functionals in the all-electron

CI calculations. Since our CI program is designed to be independent of the DFT-SCF process, it is possible to make the combination with any one-electron calculation code. Here we report the all-electron CI results employing a molecular orbital program using Slater-type orbitals as basis functions as implemented in ADF (Amsterdam density functional) code [15]. In this code, the relativistic effects are evaluated within the zeroth-order regular approximation (ZORA) using two-component relativistic wavefunctions. This is an approximated way of using four-component relativistic wavefunctions to solve the Dirac equations. ZORA is known to be accurate in the computation of the magnitude of the spin–orbit coupling [16–19]. A recent work demonstrated that Ti-2p core excitation spectra of tetravalent Ti complexes can be satisfactorily reproduced by time-dependent DFT calculations using ZORA [20]. Since we used the four-component relativistic wavefunctions to solve the Dirac equations in our previous works, we can examine the validity of the use of ZORA for the CI calculations of 3d TM $L_{2,3}$ XANES in the present study.

Here, we have selected three TM mono-oxides with a rocksalt structure, i.e. MnO, FeO and CoO as benchmark systems. After discussing the reproducibility of experimental TM $L_{2,3}$ XANES by the present method, we examine the dependence of the theoretical spectra on the quality of one-electron basis functions and exchange–correlation functionals.

2. Computational details

Relativistic CI calculations for TM-$L_{2,3}$ XANES of MnO (d^5), FeO (d^6) and CoO (d^7) were made using model clusters which are composed of one TM ion and six coordinated oxide ions. Atomic positions were obtained from the experimental crystal structures [21–23]. The point group symmetry of the model clusters is O_h and the bond length between metal and oxygen of MnO, FeO and CoO is 2.223 Å, 2.163 Å and 2.132 Å, respectively. The total numbers of electrons in model clusters were determined from formal charges of the ions. Therefore all the clusters can be expressed as $TMO_6{}^{10-}$.

At first, relativistic molecular orbital calculations were carried out by the ADF2006.01 code [15] with the ZORA. The one-electron Hamiltonian, $h(\mathbf{r})$, in ZORA is expressed as

$$h^{\mathrm{ZORA}}(\mathbf{r}) = \boldsymbol{\sigma}\cdot\mathbf{p}\frac{c^2}{2c^2 - (v_{\mathrm{nuc}}(\mathbf{r}) + v_{\mathrm{e}}(\mathbf{r}))}\boldsymbol{\sigma}\cdot\mathbf{p} + v_{\mathrm{nuc}}(\mathbf{r}) + v_{\mathrm{e}}(\mathbf{r}), \tag{1}$$

where $\boldsymbol{\sigma} = (\sigma_x, \sigma_y, \sigma_z)$ are Pauli's spin matrices, $v_{\mathrm{nuc}}(\mathbf{r})$ is the electrostatic potential from nuclei and $v_{\mathrm{e}}(\mathbf{r})$ is the Coulomb and exchange–correlation potentials from the other electrons [16–19]. Since $h(\mathbf{r})$ holds a 2×2 matrix, the eigenfunctions of $h(\mathbf{r})$ have two components. The first term of $h(\mathbf{r})$, which is the kinetic energy operator, contains the Coulomb and exchange–correlation potential operator $v_{\mathrm{e}}(\mathbf{r})$. Thus we need to solve these equations self-consistently in principle. However, it is prohibitively time-consuming. In the present calculations, $v_{\mathrm{nuc}}(\mathbf{r})$ and $v_{\mathrm{e}}(\mathbf{r})$ inside the kinetic energy operator were replaced by the sum of the potentials of the neutral spherical reference atoms V_{SA}. This procedure is called the sum of atoms potential approximation [16]. The Vosko–Wilk–Nusair (VWN) functional or the Xα functional ($\alpha = 0.7$) for the local density approximation (LDA) were used as the exchange–correlation term. An MO was expressed as the linear combination of Slater-type orbitals (STO). In the present work, we made a series of MO calculations using five different basis sets, i.e. single-ζ (SZ), double-ζ (DZ), DZ augmented with a set of polarization functions (DZP), triple-ζ augmented with a set of polarization functions (TZP) and triple-ζ augmented with two sets of polarization functions (TZ2P) for all atoms. These basis sets were supplied with the code [24]. Core orbitals were explicitly considered in the self-consistent calculations.

After the DFT-SCF calculations, the all-electron CI calculations were made. The many-electron Hamiltonian is described as

$$H = \sum_{i=1}^{N}\left[h^{\mathrm{ZORA}}(\mathbf{r}_i) - v_{\mathrm{e}}(\mathbf{r}_i)\right] + \sum_{i=1}^{N}\sum_{j<i}\frac{1}{|\mathbf{r}_i - \mathbf{r}_j|}. \tag{2}$$

The many-electron wavefunctions are expanded as linear combinations of Slater determinants as given by

$$\Psi_i = \sum_{p=1}^{M} C_{ip}\Phi_p, \tag{3}$$

where Ψ_i is the ith many-electron wavefunction, Φ_p is the pth Slater determinant, C_{ip} is its coefficient and M is the number of Slater determinants. In our previous TM $L_{2,3}$ XANES calculations, Slater determinants were constructed only from the MOs that are mainly composed of TM-2p, 3d and O-2p orbitals [9]. The electronic interactions to the other electrons were treated within the framework of DFT. In the present work, all MOs obtained by the DFT-SCF calculations were considered explicitly to construct the Slater determinants. In other words, all-electron CI calculations were performed.

The CI method in which all of the available determinants are included in the variational procedure is called full CI. Although the full CI is the most accurate method within the given MO basis set, it is prohibitively expensive in most cases. A common approximation to the full CI is the truncation of the Slater determinants at various levels of excitations. In the case of TM $L_{2,3}$ XANES, only one electron is excited from the 2p core orbitals. So we merely consider the determinants with $(\mathrm{TM\text{-}2p})^6(\mathrm{TM\text{-}}\phi_{3\mathrm{d}})^N$ configuration for the initial state and $(\mathrm{TM\text{-}2p})^5(\mathrm{TM\text{-}}\phi_{3\mathrm{d}})^{N+1}$ configuration for the final states, where N is the number of 3d electrons in the initial state. Then, the other electrons, namely TM-1s, 2s, 3s, 3p and O-1s, 2s, 2p electrons, are assumed to be fully occupied throughout the absorption process.

After diagonalizing the many-electron Hamiltonian matrix, we calculated the oscillator strengths of the absorption. Regarding the 3d TM $L_{2,3}$ XANES, the absorption process reflects the electric dipole transition from TM-2p core orbitals to TM-3d orbitals. The oscillator strength of the electric dipole transition averaged over all directions was evaluated by

$$I_{if} = \tfrac{2}{3}(E_f - E_i)\left|\langle\Psi_i|\sum_{k=1}^{n}\mathbf{r}_k|\Psi_j\rangle\right|^2, \tag{4}$$

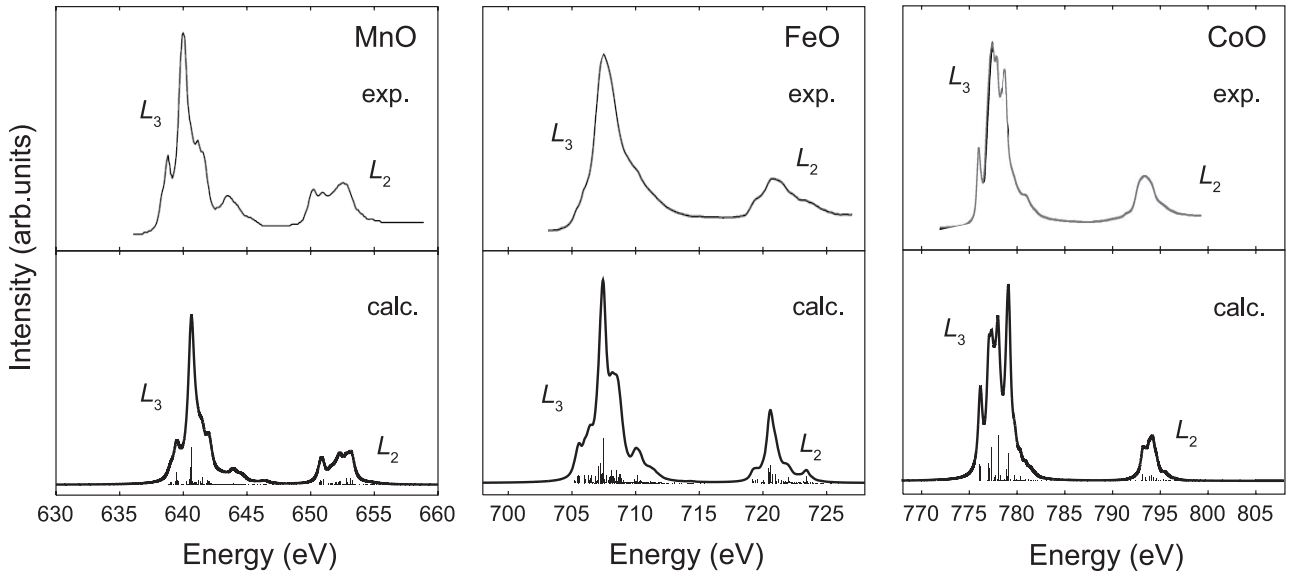

Figure 1. Theoretical TM $L_{2,3}$ XANES in comparison to experimental spectra. (TZ2P and VWN).

where Ψ_i and Ψ_j are many-electron wavefunctions for the initial state and the final state with energies of E_i and E_j. The calculated oscillator strengths were broadened by the Lorentzian function with a full width at half-maximum of 0.5 eV. This CI method is known to overestimate the absolute absorption energy systematically. This can be ascribed to the truncation of the Slater determinants, or the lack of minor contribution of the electronic correlations. In the present study, we have evaluated the absolute absorption energy from Slater's transition state of the one-electron calculations. The detail of the calculation technique was described elsewhere [7].

3. Results and discussions

Relativistic molecular orbital (MO) calculations were carried out for MnO, FeO and CoO using TMO_6 clusters within ZORA. We used TZ2P basis sets and the VWN potential for those calculations. Then, the all-electron CI calculations for TM $L_{2,3}$ XANES were carried out using the two-component MOs. First we discuss about the initial states for TM $L_{2,3}$ XANES. The numbers of Slater determinants of MnO (d^5), FeO (d^6) and CoO (d^7) for initial states, which depend on the number of combinations of d electrons' allocation, are 252 ($=_{10}C_5$), 210 ($=_{10}C_6$) and 120 ($=_{10}C_7$), respectively. Under O_h symmetry, the degenerate d orbitals are divided into triply degenerated t_{2g} orbitals and doubly degenerated e_g orbitals in the non-relativistic description. We classified the Slater determinants according to the occupation numbers of t_{2g} orbitals and e_g orbitals for simplicity. In MnO, the 252 Slater determinants are classified into five configurations, namely $(t_{2g})^5(e_g)^0$, $(t_{2g})^4(e_g)^1$, $(t_{2g})^3(e_g)^2$, $(t_{2g})^2(e_g)^3$ and $(t_{2g})^1(e_g)^4$ configurations. Considering the orthonormality of the Slater determinants, the composition of the pth Slater determinant of the ith many-electron wavefunction is given by $|C_{ip}|^2$. In table 1, the compositions of the electronic configurations at the ground states are listed. The present results are consistent with the results obtained by the DFT-CI calculations using four-component MOs [9]. All ground states are mainly composed of high spin states, namely $(t_{2g})^3(e_g)^2$ for MnO, $(t_{2g})^4(e_g)^2$ for FeO and $(t_{2g})^5(e_g)^2$ for CoO. The major spin states are consistent with those reported by experiments. In MnO and FeO, the contributions of the other configurations to the ground states are about 3%. In contrast, in CoO, that of the $(t_{2g})^4(e_g)^3$ configuration is 11%. The inclusion of different configurations as a result of CI is more important for the ground state of CoO.

Table 1. Composition of each configuration at the ground state for three TM mono-oxides.

	Configuration	Composition (%)
MnO	$(t_{2g})^5(e_g)^0$	0.0
	$(t_{2g})^4(e_g)^1$	2.1
	$(t_{2g})^3(e_g)^2$	96.8
	$(t_{2g})^2(e_g)^3$	1.1
	$(t_{2g})^1(e_g)^4$	0.0
FeO	$(t_{2g})^6(e_g)^0$	0.0
	$(t_{2g})^5(e_g)^1$	1.3
	$(t_{2g})^4(e_g)^2$	96.7
	$(t_{2g})^3(e_g)^3$	2.0
	$(t_{2g})^2(e_g)^4$	0.0
CoO	$(t_{2g})^6(e_g)^1$	0.0
	$(t_{2g})^5(e_g)^2$	88.9
	$(t_{2g})^4(e_g)^3$	11.0
	$(t_{2g})^3(e_g)^4$	0.0

Figure 1 shows theoretical TM $L_{2,3}$ XANES of three oxides and the oscillator strengths of electric dipole transitions calculated by the CI using the two-component relativistic MOs. They are compared with the experimental spectra reproduced from [25, 26]. The numbers of final states of MnO, FeO and CoO are 1260 ($=_6C_5 \times {}_{10}C_6$), 720 ($=_6C_5 \times {}_{10}C_7$) and 270 ($=_6C_5 \times {}_{10}C_8$), respectively. The theoretical spectra by

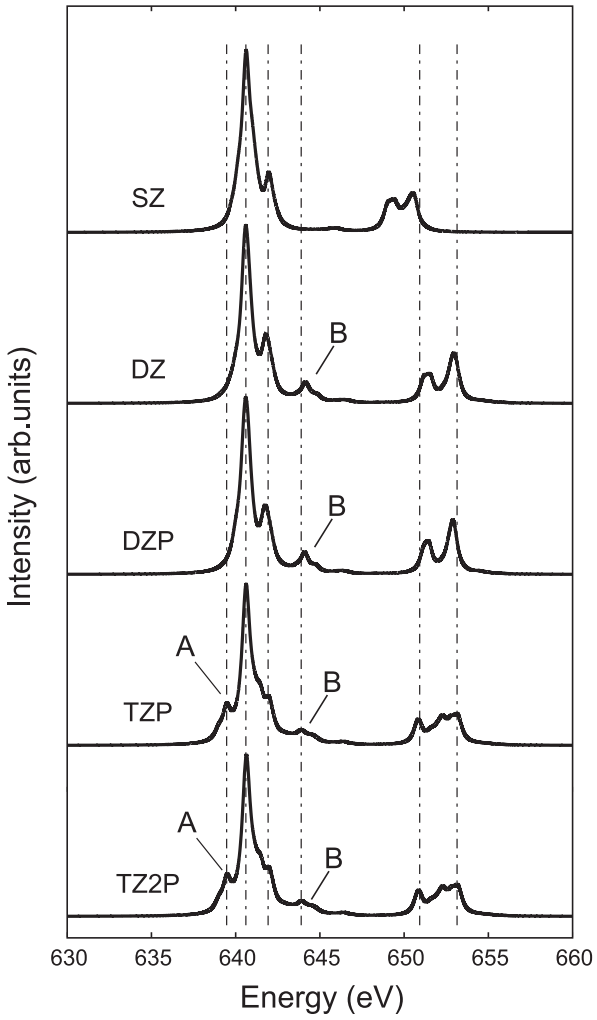

Figure 2. Dependence of the theoretical Mn $L_{2,3}$ XANES of MnO on the one-electron basis set. All spectra are shifted so as to align the main peak to that of the TZ2P spectrum. The dashed–dotted lines are guides for the eyes.

ZORA show good agreement with the experimental spectra. The characteristic features, such as relative peak positions and relative intensities, are well reproduced. The splitting between L_3 and L_2 edges can mainly be ascribed to the spin–orbit coupling of core 2p orbitals, ζ_{2p}. The calculated L_3–L_2 splitting by ZORA is quite close to that of the experimental spectra. The results suggest that the ζ_{2p} is well evaluated by ZORA. The absolute values of transition energies are also well evaluated by Slater's transition-state calculations. Note that the energy scales of the theoretical spectra are absolute values not aligned to experimental spectra. The discrepancies between the theory and the experiment are less than 1 eV.

A real intensity ratio of L_3 peak to the sum of that for L_3 and L_2 peaks, i.e. branching ratio, have been used to correlate to the valence and spin state of the TM ions [27–32]. Thole and van der Laan have discussed the branching ratio in detail [5]. They have concluded that the branching ratio is determined by the electrostatic interaction between core hole and valence electrons. The spin–orbit coupling of core 2p orbitals and that of the 3d orbitals are also important. In our

Table 2. Calculated branching ratios for three TM mono-oxides.

	Branching ratio
MnO	0.755
FeO	0.780
CoO	0.856

calculations, these values are evaluated in a first-principles manner. Table 2 lists the branching ratios obtained in the present study. All of them are larger than the statistical ratio, namely $I(L_3)/[I(L_3) + I(L_2)] = 0.67$, and it increases as the atomic number of TM increases. These results are consistent with those in the literature in experiments and theory [9, 27, 28].

CI calculations are carried out with a finite number of molecular orbitals and restricted electronic configurations. Thus the many-electron eigenvalues and eigenstates depend on the quality of MOs used in the CI calculation. In order to investigate the dependence of the $L_{2,3}$ XANES on MOs, we have carried out a series of CI calculations using MOs calculated with different atomic basis sets. Figure 2 shows the theoretical Mn $L_{2,3}$ XANES calculated using different STO basis set, i.e. SZ, DZ, DZP, TZP and TZ2P. VWN functionals were used for the exchange–correlation potential. We take the spectrum shown in figure 1 as the reference. All the other spectra were shifted so as to align with the main peak at the L_3 edge in the reference spectrum. One can see that the theoretical spectrum obtained with the TZP basis set has almost the same shapes with the reference spectrum. On the other hand, the shapes of the other three spectra are far from that of the reference. As can be seen in figure 2, when DZP and DZ basis sets are used, the sub-peak A located at the lower energy side of the L_3 main peak vanishes and the L_2 edge shows double peak features. In addition to them, when the SZ basis set is used, the satellite peaks B located at the higher energy region at the L_3 edge also vanish and the L_3–L_2 splitting becomes about 3 eV smaller than that of the reference spectrum. The results clearly indicate that the TM $L_{2,3}$ XANES strongly depends on the quality of the basis set in one-electron calculations. We can explain these dependences from the point of the quality of the MOs. The MO calculations using SZ, DZ and DZP are considered not to incorporate the chemical bonds between Mn and O sufficiently due to the small number of basis functions. As a result of this, the calculated spectra do not reproduce the experimental features well. In SZ calculations, not only the chemical bonds but also the core orbitals are not calculated properly because of the quite limited number of basis functions. The dependence of the Mn $L_{2,3}$ XANES on the exchange–correlation potentials are shown in figure 3. Two theoretical spectra shown in figure 3 were calculated using the Xα potential ($\alpha = 0.7$) and VWN potential, respectively, with a TZ2P basis set. As can be seen, the calculated spectrum using Xα potential is almost the same as that using the VWN potential. The dependence of the multiplet structure at TM $L_{2,3}$ XANES on the exchange–correlation functionals in MO calculations is much smaller than that of the basis function in the present case.

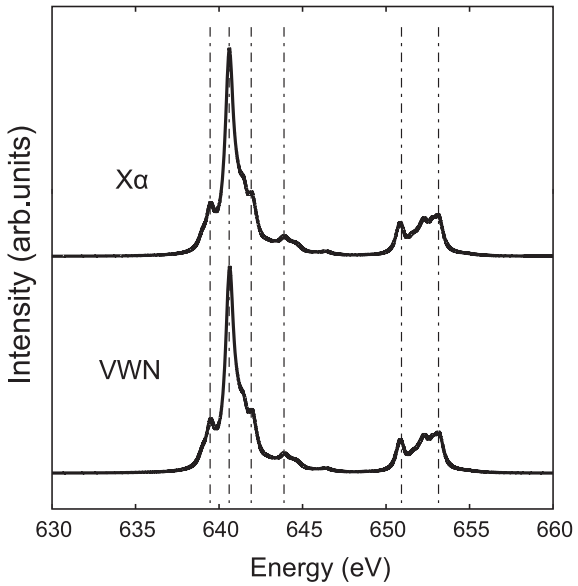

Figure 3. Dependence of the theoretical Mn $L_{2,3}$ XANES of MnO to the exchange–correlation functional. Results with VWN and Xα($\alpha = 0.7$) functionals are compared. The Xα spectrum is shifted so as to align the main peak of L_3 edge to that of the VWN spectrum. The dashed–dotted lines are guides for the eyes.

4. Summary and conclusions

All-electron CI calculations for the TM $L_{2,3}$ XANES of three 3d TM mono-oxides, namely MnO, FeO and CoO, have been made using two-component relativistic MOs. The relativistic effects were incorporated by ZORA. In addition to the discussion of the reproducibility of the experimental TM $L_{2,3}$ XANES, we also examined the dependence of the theoretical spectra on the quality of one-electron basis sets and exchange–correlation functionals. The results can be summarized as follows.

(1) The ground states of three compounds are mainly composed of high spin configurations. The major spin states are consistent with those reported by experiments. In CoO, the contribution of the second dominant configuration, $(t_{2g})^4(e_g)^3$ is 11%. The inclusion of different configurations is more important for the ground state of CoO rather than for those of MnO and FeO.

(2) All-electron CI calculations incorporating the relativistic effects through ZORA reproduced the relative positions, relative intensities and L_3–L_2 splittings observed in experimental spectra. The absolute absorption energies were also well evaluated by Slater's transition-state calculations.

(3) The calculated branching ratios are larger than the statistical ratio and increase with the atomic number of TM. These results are consistent with those in the literature both by experiments and theory.

(4) The theoretical Mn $L_{2,3}$ XANES of MnO strongly depends on the quality of the basis set in MO calculations. On the other hand, the dependence of the Mn $L_{2,3}$ XANES on the exchange–correlation functionals in MO calculations is much smaller than that of the basis function.

Acknowledgments

This work was supported by a Grant-in-Aid for Scientific Research on Priority Areas 'Nano Materials Science for Atomic Scale Modification 474' from the Ministry of Education, Culture, Sports, Science and Technology (MEXT) of Japan. YK thanks the Japan Society for the Promotion of Science (JSPS) for their research fellowship.

References

[1] de Groot F M F 2005 *Coord. Chem. Rev.* **249** 31
[2] de Groot F M F 2001 *Chem. Rev.* **101** 1779
[3] de Groot F M F 1994 *J. Electron Spectrosc. Relat. Phenom.* **67** 529
[4] de Groot F M F, Fuggle J C, Thole B T and Sawatzky G A 1990 *Phys. Rev.* B **42** 5459
[5] Thole B T and van der Laan G 1988 *Phys. Rev.* B **38** 3158
[6] Waddington W G, Rez P, Grant I P and Humphreys C J 1986 *Phys. Rev.* B **34** 1467
[7] Ogasarawa K, Iwata T, Koyama Y, Ishii T, Tanaka I and Adachi H 2001 *Phys. Rev.* B **64** 115413
[8] Ikeno H, Tanaka I, Miyamae T, Mishima T, Adachi H and Ogasawara K 2004 *Mater. Trans.* **45** 1414
[9] Ikeno H, Mizoguchi T, Koyama Y, Kumagai Y and Tanaka I 2006 *Ultramicroscopy* **106** 970
[10] Ikeno H, Tanaka I, Koyama Y, Mizoguchi T and Ogasawara K 2005 *Phys. Rev.* B **72** 75123
[11] Tanaka I, Mizoguchi T and Yamamoto T 2005 *J. Am. Ceram. Soc.* **88** 2013
[12] Kumagai Y, Ikeno H, Oba F, Matsunaga K and Tanaka I 2008 *Phys. Rev.* B **77** 155124
[13] Sonoda S, Tanaka I, Ikeno H, Yamamoto T, Oba F, Araki T, Yamamoto Y, Suga K, Nanishi Y, Akasaka Y, Kindo K and Hori H 2006 *J. Phys.: Condens. Matter* **18** 4615
[14] Hayashi H, Huang R, Ikeno H, Oba F, Yoshioka S, Tanaka I and Sonoda S 2006 *Appl. Phys. Lett.* **89** 181903
[15] Te Velde G, Bickelhaupt F M, Baerends E J, Fonseca Guerra C, van Gisbergen S J A, Snijders J G and Ziegler T 2001 *J. Comput. Chem.* **22** 931
[16] Politzer P 2002 *Relativistic Electronic Structure Theory, Part 1: Fundamentals* vol 11 (Amsterdam: Elsevier) p 622
[17] van Lenthe E, Ehlers A and Baerends E J 1999 *J. Chem. Phys.* **110** 8943
[18] van Lenthe E, Baerends E J and Snijders J G 1994 *J. Chem. Phys.* **101** 9783
[19] van Lenthe E, Baerends E J and Snijders J G 1993 *J. Chem. Phys.* **99** 4597
[20] Fronzoni G, Stener M, Decleva P, Wang F, Ziegler T, van Lenthe E and Baerends E J 2005 *Chem. Phys. Lett.* **416** 56
[21] Sasaki S, Fujino K, Takeuchi Y and Sadanaga R 1980 *Acta Crystallogr.* **A36** 904
[22] Fjellvåg H, Grønvold F and Stølen S 1996 *J. Solid State Chem.* **124** 52
[23] Liu J F, Yin S, Wu H P, Zeng Y W, Hu X R, Wang Y W, Lv G L and Jiang J Z 2006 *J. Phys. Chem.* B **110** 21588
[24] van Lenthe E and Baerends E J 2003 *J. Comput. Chem.* **24** 1142
[25] Lee H J, Kim G, Kim D H, Kang J-S, Zhang C L, Cheong S-W, Shim J H, Lee S, Lee H, Kim J-Y, Kim B H and Min B I 2008 *J. Phys.: Condens. Matter* **20** 295203
[26] Regan T J, Ohldag H, Stamm C, Nolting F, Lüning J, Stöhr J and White R L 2001 *Phys. Rev.* B **64** 214422
[27] van der Laan G and Thole B T 1991 *Phys. Rev.* B **43** 13401
[28] de Groot F M F, Hu Z W, Lopez M F, Kaindl G, Guillot F and Tronc M 1994 *J. Chem. Phys.* **101** 6570
[29] Pearson D H, Fultz B and Ahn C C 1988 *Appl. Phys. Lett.* **53** 1405
[30] Paterson J H and Krivanek O L 1990 *Ultramicroscopy* **32** 319
[31] Kurata H and Colliex C 1993 *Phys. Rev.* B **48** 2102
[32] Koshino M, Kurata H, Isoda S and Kobayashi T 2000 *Micron* **31** 373